Estimation of Complex Permittivities of Three-Dimensional Inhomogeneous Biological Bodies

DEEPAK K. GHODGAONKAR, OM P. GANDHI, FELLOW, IEEE, AND MARK J. HAGMANN, MEMBER, IEEE

Abstract—**Complex permittivities are estimated for a 36-cell model which represents the chest portion of the block model of man by using moment-method formulation of the electric field integral equation. The errors in the calculated complex permittivities are lower with saline/water as the surrounding medium, as compared to air, presumably on account of better matching of energy to the biological body. It has been shown that the rest of the human body has little effect on the estimation of complex permittivities because of the near-field nature of the illuminating sources. A small number of buried cells can be handled for solving the inverse problem, but the problem becomes ill-posed and unsolvable for a larger number of buried cells.**

I. INTRODUCTION

ELECTROMAGNETIC imaging offers promise in biomedical applications because of the relative safety of nonionizing radiation as opposed to X-rays, radioactive isotopes, etc., and a large difference in dielectric properties of cancerous and normal tissues, in general, depending upon their water content [1], [2]. In particular, there is a need for more accurate imaging of the chest cavity where large discontinuities at lung surfaces limit the use of ultrasound, and low densities limit the use of X-rays [3]. Another use of the information on the spatial distribution of complex permittivities (ϵ^*s) would be to allow individualizing the electromagnetic hyperthermia regimens for cancer therapy. Electromagnetic imaging may also have wider applications, e.g., for nondestructive testing, geophysical exploration, etc.

Whereas in X-ray imaging techniques, the propagating beam is well-collimated and therefore easy to manipulate, the electromagnetic propagation in and scattering from inhomogeneous bodies is quite complicated. The vector fields are subject to diffraction and scattering. Some of the approaches taken for solving these kinds of inverse problems are discussed in a special issue (Mar. 1981) of the IEEE TRANSACTIONS ON ANTENNAS AND PROPAGATION. A review of this issue reveals that fairly simplistic and relatively nonrealistic structures have been considered to date. Some examples are a layered medium [4], a perfectly conducting cylinder [5], and a lossless dielectric cylinder [6]. We have conducted a computer simulation of the problem using the moment-method solution of the electric field integral equation (EFIE) [7] to calculate the scattered fields ($\vec{E}^s$—magnitudes and phases) at points outside the arbitrary lossy dielectric bodies as a result of illumination from a localized near-field short dipole. The errors in the estimation of the ϵ^*s are studied as a result of the measurement errors introduced in $\vec{E}$ (total field), the dielectric properties of the surrounding medium (saline or water vis à vis air), etc. It is shown that lower errors in estimated ϵ^*s are obtained for saline/water as the surrounding medium as against air, presumably on account of a closer matching to the average dielectric properties, and hence better coupling to the biological scatterer. Also, for smaller bodies with few buried cells, the ϵ^*s can be estimated with a fair amount of accuracy (≥ 95 percent) for cell sizes considerably less than a free-space wavelength (cell size typically on the order of $\lambda_0/25$ or $0.4\ \lambda_\epsilon$), obviating therefore the restrictions imposed by Rayleigh criterion which is valid strictly for far-field problems.

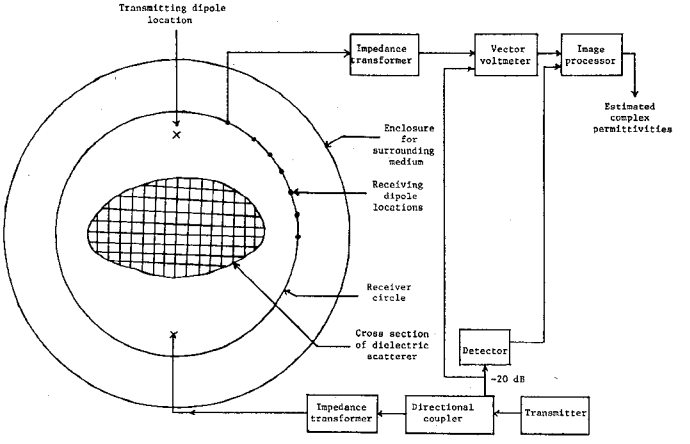

Fig. 1. A conceptual layout of the device.

II. RF ELECTROMAGNETIC "IMAGING" SYSTEM

A conceptual layout of the proposed "imaging" system is shown in Fig. 1. Receiving dipoles are located at various positions on the circle, while the transmitting dipoles acting one at a time are located at the front and back positions as shown in Fig. 1. These locations of the transmitting and receiving dipoles are repeated at several positions along the major axis, which is perpendicular to the

Manuscript received September 7, 1982; revised February 7, 1983.

D. K. Ghodgaonkar and O. P. Gandhi are with the Department of Electrical Engineering, University of Utah, Salt Lake City, UT 84112.

M. J. Hagmann is with the National Institutes of Health, Bethesda,

0018-9480/83/0600-0442$01.00 ©1983 IEEE

two-dimensional cross section of the scatterer. When one of the transmitting dipoles is excited by the transmitter, the received electric field (magnitude and phase for the three orthogonal components) is measured at each of the receiving dipole locations. This procedure is repeated for all the locations of the transmitting dipoles. In our formulation, it is necessary to measure the scattered fields at N locations, where N equals the number of cell centroids of the inhomogeneous body where the ϵ^*s are to be estimated. The image processor solves for the ϵ^*s for each of the cells of the body for each location of the transmitting dipoles, ignoring the calculated values for any of the cells if the real and imaginary parts ϵ_R and ϵ_I, respectively, do not fall within the limits $1 \leqslant \epsilon_R \leqslant 100$ and $0 \leqslant \epsilon_I \leqslant 200$. These limits are, of course, selected from the *a priori* knowledge of the bounds of the values that can possibly occur. The average of the complex permittivities for the various cells is the output that is provided.

Back coupling from the dielectric scatterer to the transmitting and receiving dipoles is neglected in the formulation of the problem. Typically, short dipoles ($2h \simeq 0.1\ \lambda_\epsilon \simeq 2$ cms, where λ_ϵ is the wavelength in the surrounding medium) are contemplated for this application. It has been shown experimentally in our laboratory that the feed point impedances of such short dipoles are altered by less than 5 percent by placement of biological-phantom-filled bodies at distances larger than $2h$—a condition that is planned for the proposed scheme.

III. Matrix Formulation for Forward and Inverse Problems

The forward problem needs only to be solved for computer simulation of the proposed scheme, since it is assumed that the measured values of the scattered fields will be an errored version of these values.

The scattered fields $\vec{E}_2^s$ at N receiving dipole locations are related to the actual internal fields $\vec{E}_1$ at the cell centroids of the scattering body through the relationship

$$\vec{E}_2^s = \vec{\vec{B}} \cdot \vec{E}_1 \tag{1}$$

where the Green's function matrix $\vec{\vec{B}}$ is a $3N \times 3N$ matrix corresponding to the 3 components of the electric field for each of the N locations.

The actual electric fields $\vec{E}_1$ at each of the N cell centroids are in turn given from the incident electric fields $\vec{E}_1^i$ at the corresponding location by the moment-method formulation [8]

$$\vec{\vec{A}} \cdot \vec{E}_1 = -\vec{E}_1^i. \tag{2}$$

In the inverse problem, the objective is to calculate complex permittivities for different cells from the knowledge of measured electric fields at all the receiving dipole locations and calculated incident fields at the cell centroids ($\vec{E}_1^i$) and receiving dipole locations ($\vec{E}_2^i$). The matrices $\vec{\vec{A}}$ and $\vec{\vec{B}}$ can be factorized [9] as

$$\vec{\vec{A}} = \vec{\vec{A}}_1 \cdot \vec{\vec{R}} - \vec{\vec{I}} \tag{3}$$

$$\vec{\vec{B}} = \vec{\vec{B}}_1 \cdot \vec{\vec{R}} \tag{4}$$

where $\vec{\vec{A}}_1$ and $\vec{\vec{B}}_1$ depend on frequency, cell size and location, and locations of receiving dipoles, $\vec{\vec{I}}$ is the identity matrix, and $\vec{\vec{R}}$ is a diagonal matrix containing only the values of $(\epsilon_r^* - 1)$ for the various cells.

Using (1)–(4), we obtain

$$\vec{\vec{R}}^{-1} \cdot \vec{\vec{B}}_1^{-1} \cdot \vec{E}_2^s = \vec{\vec{A}}_1 \cdot \vec{\vec{B}}_1^{-1} \cdot \vec{E}_2^s + \vec{E}_1^i. \tag{5}$$

The above equation solves the inverse problem by taking the ratio of the corresponding elements in the two column vectors. The objective of this inverse scattering approach is to end up with tolerable errors (say within ± 5 percent) in the estimated ϵ^*s for realistic experimental errors introduced in the total electric field ($\vec{E}_2^i + \vec{E}_2^s$) at the various dipole locations. It is assumed that multiple redundant measurements would help in reducing the effective experimental errors in the measured data, which would result in better estimates of the dielectric properties. To achieve this in actual practice, it is envisaged that the needed N projections for the electric fields at N locations of receiving dipoles would be obtained from measurements at more than N locations by using the Fourier series interpolation and the fast Fourier transform technique. A large number of measurements could, for example, be taken by measuring at smaller angular intervals.

To allow for a large number of cells, it is observed that the storage requirements and the computation time for formation and factorization of matrix $\vec{\vec{B}}_1$ in (5) should be reduced. If the biological body and the receiver configuration used for solving inverse problems are symmetric, then the matrix $\vec{\vec{B}}_1$ can be block diagonalized, which results in considerable savings in computer time and storage [10], [11]. Because the dielectric properties of saline/water are very close to that of a biological body, any arbitrary shaped body can be made symmetric by extending it into saline/water for the purpose of solving inverse problems. In general, the shape of the extended biological body is like a parallelepiped which has one or two or three planes of symmetries, depending on the size and location of cells and the receiver location. By this block diagonalization technique, the storage requirements and the formation time are approximately reduced by a factor of 2^n, and the factorization time is reduced by a factor of 2^{2n}, where n is the number of planes of symmetries.

IV. Numerical Results

A body studied at length is a 36-cell ($4 \times 3 \times 3$) model of the human chest cavity shown in Fig. 2. The overall dimensions of the body are $30 \times 22.5 \times 22.5$ cm, with the cell numbering also given in Fig. 2. The values of the complex permittivities used for the various cells for the direct problem are given in Table I. These values (without parentheses) have been obtained from the volume-averaged dielectric properties for the various regions of the chest cavity from the anatomical data [12] on the composition of the tissues (fat, muscle, skin, bone, etc.). It should be noted that organs such as the lung, liver, spleen, kidney, and heart are located in the chest cavity and are apportioned amongst the 36 cells ascribed to this volume. Also given in Table I in parentheses are the respective calculated values obtained from the inverse

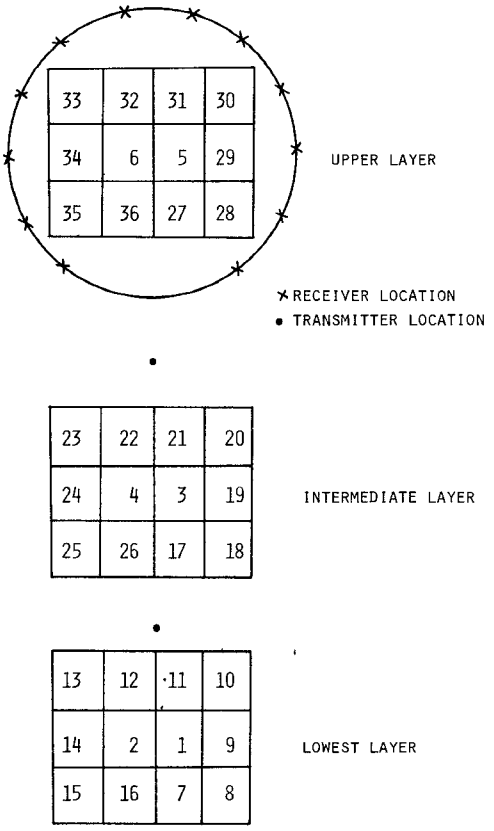

Fig. 2. The cell numbering of the three-layered 36-cell body to model the human chest cavity. The complex permittivities assumed and calculated for the various cells are given in Table I.

TABLE I
ASSUMED AND ESTIMATED COMPLEX PERMITTIVITIES FOR THE 36-CELL BODY
(The estimated values are given in parentheses.)

Cell No.	ϵ_R	ϵ_I	Cell No.	ϵ_R	ϵ_I	Cell No.	ϵ_R	ϵ_I
1	54.21 (51.16	111.31 114.53)	13	73.08 (73.15	122.48 122.28)	25	48.48 (49.33	103.54 103.97)
2	54.21 (49.15	111.31 110.67)	14	64.98 (64.21	125.33 124.67)	26	54.21 (56.64	123.16 123.89)
3	37.12 (40.15	65.00 60.48)	15	59.13 (58.29	133.64 134.12)	27	40.17 (38.34	104.67 103.05)
4	37.12 (44.58	65.00 61.43)	16	61.76 (60.37	129.64 130.13)	28	25.79 (25.45	53.49 53.09)
5	38.13 (36.98	89.48 90.01)	17	54.21 (56.72	123.16 121.63)	29	23.46 (24.12	47.21 47.26)
6	38.13 (30.54	89.48 93.99)	18	48.48 (49.24	103.54 102.64)	30	39.08 (39.26	88.31 88.22)
7	61.76 (61.57	129.65 130.80)	19	46.41 (46.14	70.87 71.97)	31	38.51 (41.50	87.53 85.38)
8	59.13 (59.14	133.64 134.10)	20	45.97 (45.45	95.89 96.25)	32	38.51 (39.99	87.53 83.98)
9	64.98 (64.01	125.33 124.85)	21	40.40 (39.70	89.37 89.12)	33	39.08 (39.01	88.31 87.78)
10	73.08 (72.97	122.48 122.56)	22	40.40 (40.89	89.37 88.20)	34	23.46 (25.77	47.21 46.72)
11	50.48 (50.41	111.0 110.99)	23	45.97 (45.66	95.89 95.28)	35	25.79 (25.18	53.49 53.38)
12	50.48 (50.87	111.00 111.32)	24	46.41 (45.23	70.87 71.56)	36	40.17 (38.28	104.67 104.64)

problem assuming Gaussian errors with standard deviation in magnitude of 0.01 percent and a standard deviation in phase of 0.002° in the total fields ($\vec{E}_2^i + \vec{E}_2^s$). The other salient features assumed for the calculations given in Table I are as follows.

Frequency = 150 MHz.

Surrounding medium: 0.29-percent saline, $\epsilon^* = 76.0 - j58.3$.

Radius of the receiver circle = 19.75 cm. (Cell size = 7.5 cm (0.0375 λ_0 or 0.388 λ_ϵ) and $N = 36$.)

Number of transmitter locations = 4 (in planes intermediate to those between layers 1 and 2 and 2 and 3, respectively).

Distance of the transmitting dipoles from the center of the body = 17.5 cm.

While in this approach any frequency in the range of 50–450 MHz could have been selected, the frequency of 150 MHz was picked since it is high enough to give reasonable resolution and yet low enough to have a significant depth of penetration. For higher frequencies, a larger number of cells are needed to represent the body since the cell size must be small compared to $\lambda_{g\epsilon}/4$. Dipole size is immaterial as long as short dipoles $h \leqslant \lambda_\epsilon/10$ are used. Distance of the transmitting dipole from the center of the body is chosen so that the incident field at the nearby receiver location is comparable to the scattered field. If the incident field dominates the total fields at receiver locations, then the measurement error in total fields is amplified in the scattered fields which are used for solving inverse problems. The radius of the receiver circle should be as small as possible in order to obtain larger amplitude and phase differences in the fields received from the various cells.

As seen in Table I, the calculated average errors in ϵ^* for all locations are fairly small; 3.67 percent for the real part and 1.22 percent for the imaginary part. Somewhat larger input errors could have been tolerated for proportionately larger errors in the estimated ϵ^*s. Note that in spite of the 3:1 variability in the values of the ϵ^*s, the inverse problem is able to estimate the respective values with a fair amount of accuracy. It is to be recognized, however, that because of the ill-conditioning of the matrices, the errors in the estimated ϵ^*s are a factor of 100–300 times those encountered for the input measurements. The need for an accurate measurement of the scattered fields with or without redundant measurements must therefore be emphasized.

Since the volume to be "imaged," say the chest cavity, is a part of the entire human body, it was necessary to estimate the effect of the rest of the body on the internal $\vec{E}$-fields ($\vec{E}_1$) for the volume of interest, because it is the latter that we normally model for the inverse problem. Toward this end, the internal fields are calculated for bodies $A(24\times4\times2)$, $B(6\times4\times2)$, and $C(4\times4\times2)$ shown in Fig. 3 with 0.29-percent saline ($\epsilon_s = 76.0 - j58.3$) as the surrounding medium. For all cases, a near-field short-dipole type antenna ($2h = 0.1\ \lambda_\epsilon$, $d = 0.9\ \lambda_\epsilon$) was used as the source. Fields associated for the cells of the core body C were found to be within ±3 percent in magnitude and ±3° in phase of those calculated for bodies A and B for the same cell locations. This illustrates that with near-field sources and saline for good match with the body, it may be possible to ignore the rest of the body and concentrate only

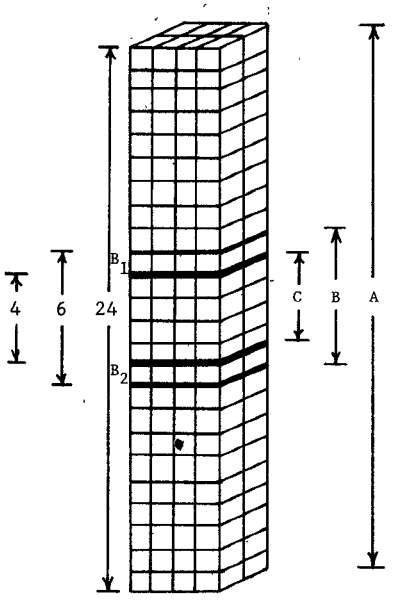

Fig. 3. Bodies *A*, *B*, and *C* represent, respectively, the whole body, the extended volume, and the volume of interest.

TABLE II
VARIATION OF AVERAGE PERCENTAGE OF ERROR IN REAL AND IMAGINARY PARTS OF COMPLEX PERMITTIVITIES WITH ϵ_s THE COMPLEX PERMITTIVITY OF THE SURROUNDING MEDIUM

Surrounding Medium	ϵ_s	$\bar{e}_R$	$\bar{e}_I$
Free space	1 - j0.0	66.4	74.2
Pure water	77.9 - j0.6	15.9	11.3
Ethylene glycol	41.0 - j60.0	4.3	1.6
0.1% saline	76.0 - j20.0	11.5	4.1
0.29% saline	76.0 - j58.3	3.9	1.5
0.37% saline	76.0 - j75.4	3.1	1.3
0.45% saline	76.0 - j92.02	2.8	1.3
0.58% saline	76.0 - j118.55	2.6	1.6

on the volume of interest, reducing thereby the number of cells that must be considered, and hence the calculation time. Because of a somewhat larger discrepancy in the fields for the peripheral cells (layers B_1, B_2 for body B), it may in practice be advantageous to consider a somewhat extended body such as body B if a larger accuracy is to be maintained for the inner region C of the body.

V. Effect of the Surrounding Medium

Table II shows the effect of the surrounding medium on the average errors $\bar{e}_R$ and $\bar{e}_I$ in the real and imaginary parts, respectively, of the calculated permittivities. The various parameters assumed are as follows.

Radius of receiver circle = 18 cm.

Number of transmitter locations = 4 (in planes intermediate to those between layers 1 and 2 and 2 and 3, respectively).

Distance of the transmitting dipole from the center of the body = 13.5 cm.

Error in measured fields: Amplitude = 0.4 percent and Phase = 0.05°.

For each of the cases, a 3×4×2-cell body is considered at a frequency of 150 MHz. Considerably lower errors are obtained for saline and ethylene glycol which match the average dielectric properties of the tissues better than does air.

TABLE III
ERRORS IN CALCULATED COMPLEX PERMITTIVITIES FOR SOME INHOMOGENEOUS BODIES

Cells in the Body	Figure	Number of Transmitter Locations	Input Error Magnitude	Input Error Phase	Number of Buried Cells	$\bar{e}_R$	$\bar{e}_I$
3 x 4 x 2		4	0.4%	0.05°	0	3.9%	1.5%
3 x 4 x 3	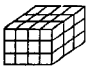	4	0.01%	0.002°	2	3.67%	1.22%
2 x 4 x 4	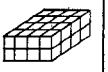	2	0.01%	0.002°	4	8.41%	2.74%

VII. Errors for Inhomogeneous Bodies with a Varying Number of Buried Cells

Table III compares the average errors in the estimated values of ϵ^*s for three illustrative bodies with a varying number of buried cells. For a body with no buried cells, considerably lower errors in the estimated values are obtained, allowing thereby large errors in the measured fields that form the input to the problem. The errors increase rapidly with an increasing number of buried cells, making it nearly impossible to estimate the ϵ^*s with a reasonable accuracy for bodies with a larger number of buried cells. This is ascribed to the nearly identical scattered fields (magnitude and phase) from the interior regions of the body and the tremendous ill-conditioning of the matrix $\overleftrightarrow{B}_1$ that results thereby.

VIII. Conclusions

A computer simulation of an electromagnetic "imaging" approach is presented for three-dimensional inhomogeneous biological bodies using the moment-method solution of the electric field integral equation to estimate the complex permittivities for the various regions of the body. It is shown that because of the near-field illumination, such as those from short dipoles, it is possible to concentrate on parts of an intact body. ϵ^*s can be estimated with reasonable accuracies for cell sizes on the order of $\lambda_0/25$ which are a fraction of λ_ϵ within the tissues. It is necessary, however, to measure the scattered field (magnitude and phase) with a great deal of accuracy. Multiple redundant measurements with Fourier series interpolations may help toward this end. For biological bodies, lower errors in estimated ϵ^*s are obtained for physiological saline/water as the surrounding media as against air, presumably on account of a closer matching, and hence better coupling to the average dielectric properties of the scatterer. A small number of buried cells are acceptable for estimation of ϵ^*s. The problem, however, becomes ill-posed with a larger number of buried cells. In spite of the pointed deficiencies

of the approach, several useful biomedical and other nondestructive applications may be possible, including an estimation of the inhomogeneous ϵ^*s for the human head as a prelude to diagnostic and hyperthermia applications.

REFERENCES

[1] C. C. Johnson and A. W. Guy, "Nonionizing electromagnetic wave effects in biological materials and systems," *Proc. IEEE*, vol. 60, pp. 692–718, 1972.

[2] E. H. Grant, Physics Department, Queen Elizabeth College, Univ. of London, London, England, personal communication.

[3] R. Maini, M. F. Iskander, and C. H. Durney, "On the electromagnetic imaging using linear reconstruction techniques," *Proc. IEEE*, vol. 68, pp. 1550–1552, 1980.

[4] S. Coen, K. K. Mei, and D. J. Angelakos, "Inverse scattering technique applied to remote sensing of layered media," *IEEE Trans. Antennas Propagat.*, vol. AP-29, pp. 298–306, 1981.

[5] D. Colton, "The inverse electromagnetic scattering problem for a perfectly conducting cylinder," *IEEE Trans. Antennas Propagat.*, vol. AP-29, pp. 364–368, 1981.

[6] A. K. Datla and S. C. Som, "On the inverse scattering problem for dielectric cylindrical scatterers," *IEEE Trans. Antennas Propagat.*, vol. AP-29, pp. 392–397, 1981.

[7] D. E. Livesay and K. M. Chen, "Electromagnetic fields induced inside arbitrary shaped biological bodies," *IEEE Trans. Microwave Theory Tech.*, vol. MTT-22, pp. 1273–1280, 1974.

[8] M. J. Hagmann, O. P. Gandhi, and C. H. Durney, "Numerical calculation of electromagnetic energy deposition for a realistic model of man," *IEEE Trans. Microwave Theory Tech.*, vol. MTT-27, pp. 804–809, 1979.

[9] M. J. Hagmann, O. P. Gandhi, and D. K. Ghodgaonkar, "Application of moment methods to electromagnetic biological imaging," in *IEEE MTT-S Int. Microwave Symp. Dig.* (Los Angeles, CA), June 15–19, 1981, p. 482.

[10] J. W. Leech and D. J. Newman, *How to Use Groups*. London, England: Methuen, 1969.

[11] R. McWeeny, *Symmetry — An Introduction to Group Theory and Its Applications*. New York: Macmillan, 1963.

[12] D. J. Morton, *Manual of Human Cross-Section Anatomy*. Baltimore, MD: Williams and Wilkins, 1944.

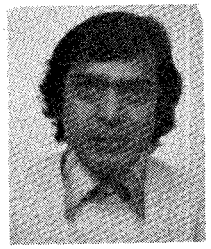

Deepak K. Ghodgaonkar was born in Jodhpur, India, on November 27, 1955. He received a B.E. degree from the University of Indore, India, in 1976, and an M. Tech. degree from the Indian Institute of Technology, Bombay, India, in 1978, both in electrical engineering.

From 1978 to 1980 he worked as a Scientific Officer in the Special Microwave Products Unit of Tata Institute of Fundamental Research, Bombay, India. He is currently a graduate student in the Department of Electrical Engineering at the University of Utah, Salt Lake City, where he is also employed as a Research Assistant.

Om P. Gandhi (S'57–M'58–SM'65–F'79) was born in Multan, West Pakistan, on September 23, 1934. He received the B.Sc. (Honors) degree in physics from Delhi University in 1952, the Diploma in electrical communication engineering from the Indian Institute of Science, Bangalore, India, in 1955, and the M.S.E. and Sc.D. degrees in electrical engineering from the University of Michigan, Ann Arbor, in 1957 and 1960, respectively.

Subsequently, he worked at Philco Scientific Laboratory, Blue Bell, PA, on semiconductor plasmas. From 1962 to 1966 he worked at Central Electronics Engineering Research Institute, Pilani, India, first as Assistant Director and then as Deputy Director in charge of the Microwave Devices group. Since 1967 he has been with the University of Utah, Salt Lake City, where he is a Professor of Electrical Engineering and Research Professor of Bioengineering. His research interests include electromagnetic biological effects and biomedical applications of microwaves.

Dr. Gandhi is a member of Sigma Xi, Phi Kappa Phi, and Eta Kappa Nu.

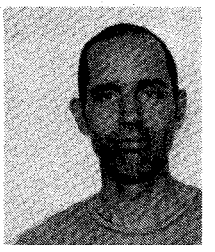

Mark J. Hagmann (S'75–M'79) was born in Philadelphia, PA, on February 14, 1939. He received the B.S. degree in physics from Brigham Young University, Provo, UT, in 1960, and the M.Sci.Ed. and the Ph.D. degree in electrical engineering from the University of Utah, Salt Lake City, in 1966 and 1978, respectively. He did additional graduate studies in physics at Brigham Young University, Provo, UT, during 1965–1967.

He worked as a Physics and Mathematics Teacher during 1961–1964. During 1968–1975 he worked in the research and development of explosives for IRECO Chemicals, West Jordan, UT. He was a Research Associate in the Departments of Electrical Engineering and Bioengineering at the University of Utah from 1978–1980. He is presently with the National Institutes of Health, Bethesda, MD.